DOI: 10.1002/ejic.200700454

An Approach to the Synthesis of Silicon Carbide Nanowires by Simple Thermal Evaporation of Ferrocene onto Silicon Wafers

Jun-Jie Niu*[a] and Jian-Nong Wang[a]

Keywords: Silicon / Carbides / Thermal evaporation / Ferrocene / Nanowires

Scales of silicon carbide nanowires (SiC-NWs) with high quality were synthesized by direct thermal evaporation of ferrocene onto silicon wafers at high temperature. Ferrocene decomposed into iron and carbon, which was subsequently treated with silicon to form SiC-NWs at high temperature. The SiC-NWs possess small diameters of ≈ 20 nm and lengths of several μms. Furthermore, the samples show a uniform morphology, crystalline structure, and a very thin oxide layer. The main crystal direction of [111] was confirmed by high-resolution field-emission-transmission electron microscopy (HR-FETEM). The Raman scattering spectra showed two peaks at ≈ 796 (TO) and ≈ 980 cm^{-1} (LO) with varying intensity ratios at different positions. The band line fluctuation was contributed to the Raman selection rules. With reference to the experimental results, we suggested a tentative growth model according to the vapor–liquid–solid (VLS) mechanism.

Introduction

Silicon carbide presents wide applications in many harsh conditions such as high temperature and high frequency due to the high mechanical strength, high chemical stability, low induced activity, and so forth.[1] Many high-performance silicon carbide based devices are now commercially available, including metal semiconductor field-effect transistors and Schottky rectifiers. One-dimensional nanomaterials deserve special attention, as they are expected to play a crucial role as building blocks of future molecular electronic applications.[2–4] Silicon carbide nanowires (SiC-NWs), possessing a special geometrical and wide band-gap semiconductor structure, show the considerable advantage of a high electrical conductance and excellent mechanical stability, which makes them extremely interesting in many electrical and mechanical fields. Much effort has been focused in the miniaturization of electronic devices by using SiC-NWs in the last decade.[5–7] It was demonstrated that the SiC-NWs displayed excellent field emission and optical properties due to their remarkable structural and chemical stabilities.[6,8–10] Furthermore, SiC-NWs also exhibit good mechanical features in reinforcing the strength of ceramic–matrix composite.[11–12]

A number of existing techniques can be used for the synthesis of SiC-NWs, including carbon nanotube confined reactions,[5,13–16] carbothermal reduction,[17–21] metal-assisted vapor–liquid–solid (VLS) growth,[8,22–25] etc. Among them, a process based upon the carbon nanotube (CNTs) solid–vapor reaction with volatile oxides and/or halide species, was reported.[5] By using the floating catalyst ferrocene with the $SiCl_4$–C_6H_6–H_2–Ar system, SiC nanorods with sizes of ≈ 100 nm were obtained.[23] If the ferrocene on the silicon wafer was reacted at 600 °C with an ultrahigh vacuum (UHV) system, SiC nanodots will be formed.[24] Lee and coworkers have synthesized crystalline β-SiC-NWs with diameters of 10–30 nm by hot filament chemical vapor deposition (HFCVD), and these nanowires possessed good field-emitting properties.[22,26] Yang et al. proposed the synthesis of SiC-NWs by the thermal decomposition of a polymeric precursor with a thickness ranging from 80 to 200 nm.[27] Needle SiC-NWs were successfully prepared by thermal evaporation of SiC powder and iron powder at a high temperature of 1700 °C.[28] Moreover, Deng et al. found that single crystalline SiC-NWs could be grown directly on the surface of bulk SiC ceramic substrates in a catalyst-assisted thermal heating process.[29] However, most of the synthetic methods involved complex processes and manipulations. Furthermore, the as-produced SiC-NWs were usually over 30 nm in size and a contained a thick oxide layer. It is desirable to fabricate crystalline SiC-NWs with small diameters that are free of oxide layers by a simple process. Furthermore, the Raman scattering spectra of SiC-NWs are seldom studied and need to be further investigated.

Herein we report an alternative approach in which scales of high-quality SiC-NWs were synthesized by the simple thermal evaporation of ferrocene onto silicon wafers. Iron as a catalyst and carbon pyrrolyzed by ferrocene at high temperatures deposited on the surface of silicon wafers and reacted with silicon to generate SiC-NWs. The as-formed

[a] School of Materials Science and Engineering, Shanghai Jiao Tong University
Shanghai 200030, P. R. China
Tel.: +86-21-62932050
E-mail: jjniu@sjtu.edu.cn

SiC-NWs with small diameters of ≈ 20 nm and lengths of several μms show a well-crystalline structure, uniform size distribution, and thin oxide layer. Furthermore, the crystal direction of [111] is clearly observed. Two peaks at ≈ 796 (TO) and ≈ 980 cm^{-1} (LO) in the Raman scattering spectra show varying intensity ratios at different positions. The intensity fluctuation is attributed to the Raman selection rules. Finally, we suggest a possible growth model that is related to the vapor–liquid–solid (VLS) mechanism.

Results and Discussion

Figure 1 displays the FESEM image of scales of SiC-NWs with diameters of ≈ 20 nm and lengths of several μms. Relatively straight SiC-NWs with uniform size distributions and smooth surfaces can be clearly observed from the enlarged image in Figure 1b. It also can be seen that the surface of the SiC-NWs is clean and free of impurities. Shown in Figure 1c is an interesting FESEM image of as-grown SiC-NWs sticking to the silicon wafer. As can be seen from the figure, the homogeneous SiC-NWs closely contact to the surface of the silicon wafer, indicating a different growth procedure relative to Figure 1a and b. The possible chemical composition of the sample was analyzed through the EDS data recorded from several pure nanowires (Figure 1d). The presence of peaks demonstrates that the nanowires are composed of silicon, carbon, and small amount of oxygen. The quantitative element analysis shows a Si/C ratio of 1:1, which corresponds well to the standard SiC (1:1) and thus confirms the composition of the SiC nanowires. The small quantity of oxygen may come from the resident oxide layer or the adsorbed oxygen in the air. The Fe peak was not detected because of the weak concentration. Shown in Figure 2 are the TEM images of several SiC-NWs with mean diameters of ≈ 20 nm and lengths of 2–3 μms. It is clear that the SiC-NWs are structurally uniform and dislocation free. We estimated the diameter distribution of the SiC-NWs by calculating hundreds of nanowires from the TEM images. As can be seen from Figure 4b, the majority of SiC-NWs show a concentrated diameter arrangement of ≈ 20 nm. Some of the SiC-NWs have sizes that are less than 10 nm and very few are over 25 nm. The high-magnification TEM image in Figure 2b more clearly shows a smooth morphology and homogeneous size distribution of the SiC-NWs. Moreover, the SiC-NWs are of high quality with free of defects such as stacking faults. The selected area electric diffraction (SAED) pattern corresponding to the SiC-NWs indicates a crystalline structure (Figure 2a inset). The (111) face that is confirmed in the figure suggests a main growth direction of [111] because of the lowest energy theory. Otherwise, the fluctuant brightness of black and white in the TEM image synchronously indicates a crystalline nature. The lattice structure of the SiC-NWs can be viewed in the HR-FETEM image (Figure 3). As can be seen from Figure 3, the regular interplanar spacing of 0.25 nm shows good agreement with SiC growth along the [111] direction, indicating a single-crystalline structure. Otherwise, it is observed that the lattice fringes are parallel to the nanowire axes, which indicates a [220] growth direction. It can also be observed that the surfaces

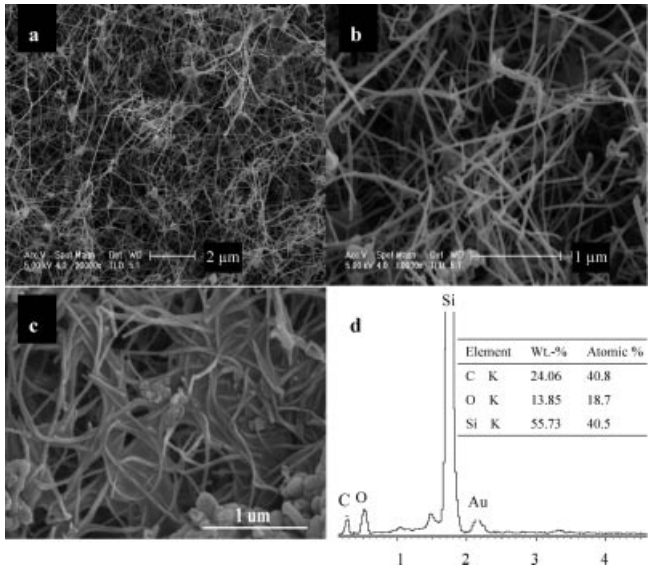

Figure 1. (a) The low-magnification, (b) high-magnification, and (c) special-structure FESEM images of the SiC-NWs with mean diameters of ≈ 20 nm and lengths of several μms. (d) The EDS spectrum and quantitative elemental analysis recorded from the pure SiC-NWs. The weak Au and unmarked peaks come from sample preparation during the FESEM measurements.

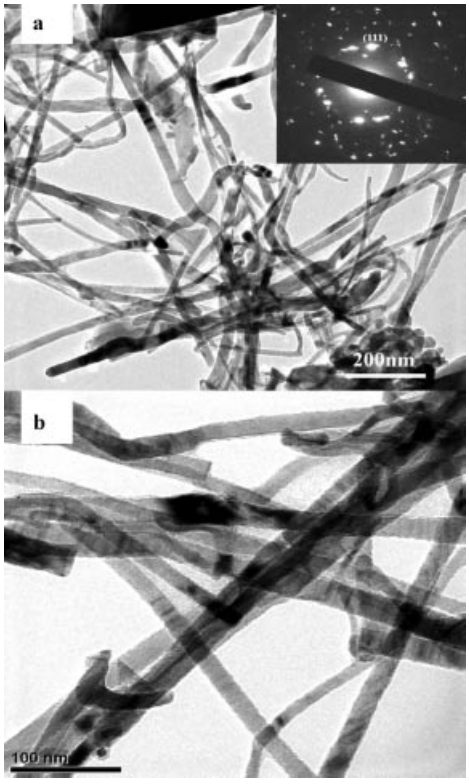

Figure 2. (a) The low-magnification and (b) high-magnification TEM images of the SiC-NWs. The inset in (a) is the corresponding SAED pattern.

of the SiC-NWs are smooth and clean and possess only a very thin oxide layer of less than 1 nm. As a result, the SiC-NWs are structurally uniform, singly crystalline, and have only a thin oxide layer.

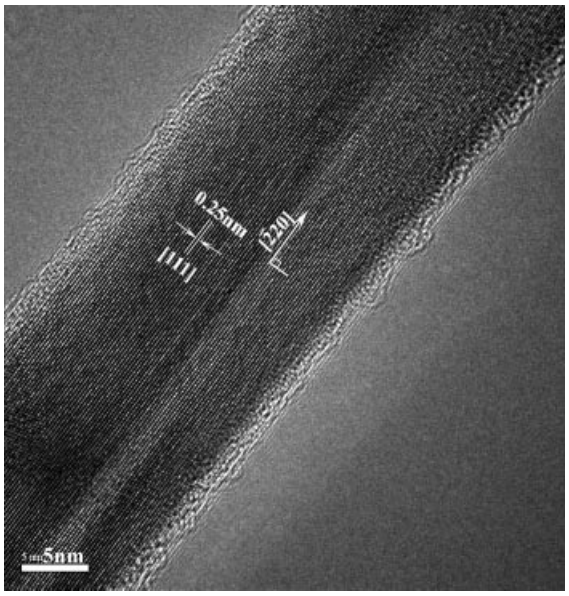

Figure 3. HR-FETEM image of a SiC-NW with the lattice orientation of [111].

Shown in Figure 4a is the XRD data of the sample, which is used for analyzing the crystalline structure. As can be seen from the pattern, the peaks of (111), (200), (220), (311), and (222) are completely consistent to the standard face-centered cubic (fcc) cell of SiC with the lattice constant of a = 0.4349 nm (JCPDS card No. 73–1665). The strong intensity and narrow width of the lines also indicate an excellent crystal structure, which is also shown in the HR-FETEM image. Except for the peaks of SiC, several peaks of Si_2N_2O with a low intensity are synchronously observed. These reflection lines are believed to be derived from weak nitrification and oxidation during the procedure.

Figure 5A displays the Raman scattering spectrum of a typical SiC-NW sample at room temperature. There is a prominent band line at ≈ 796 cm^{-1} and a low intensity line at ≈ 980 cm^{-1}; these two lines correspond well to the band lines of a zincblende structure of bulk SiC. Furthermore, these bands normally result from the first-order phonon frequencies of the transverse optical (TO) and longitudinal optical (LO) modes, respectively.[30] Between these two lines, the lines at 729 and 887 cm^{-1} can also be distinguished. These two peaks may be attributable to special SiC-NWs Raman-active modes or to impurities. As can be seen from the figure, the symmetry and narrow width of the lines indicate a crystalline nature of the high-quality SiC-NWs. The lines in this Raman spectrum are consistent with those reported for SiC nanorods or nanowires,[25,31] but they are different to those of bulk materials or films of SiC.[32–33]

It is known that the LO band line is usually higher than the TO band line near the zone center in bulk SiC.[34] However, in this Raman scattering spectrum, the TO band

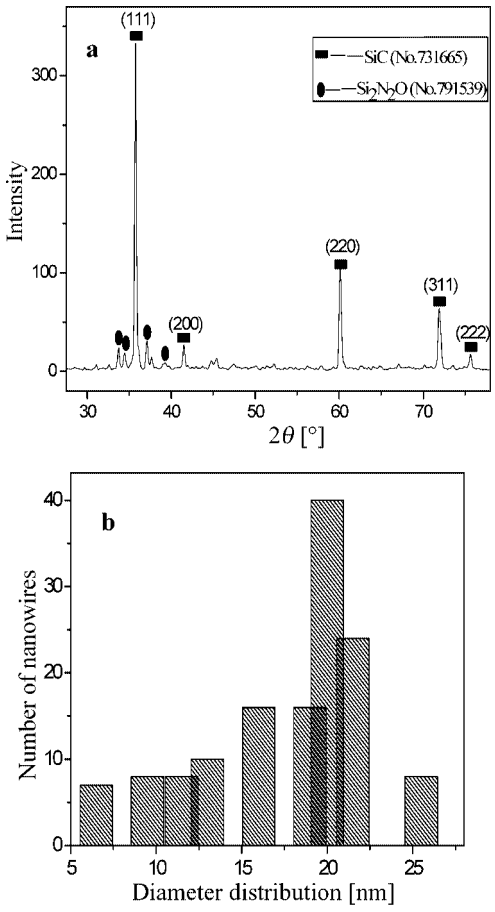

Figure 4. (a) XRD pattern of the SiC-NW sample. (b) Diameter distribution of the SiC-NWs.

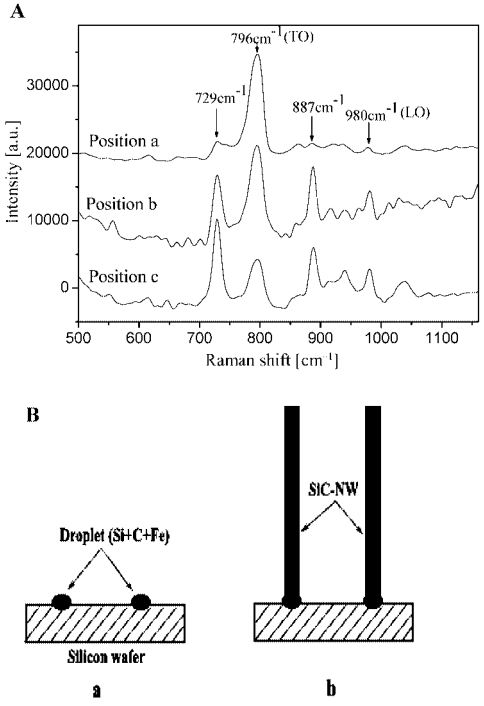

Figure 5. (A) Raman scattering spectra of the SiC-NWs with different positions. (B) Schematic illustration of the SiC-NWs growth model.

shows a stronger intensity than the LO band (Figure 5A). As depicted in the figure, the SiC-NWs sample exhibits a fluxional intensity ratio of the various band lines when it was irradiated at different positions. The intensity of the TO band at ≈ 796 cm^{-1} continually decreases whereas the LO band at ≈ 980 cm^{-1} increases when the radiation is moved from position a to c. These phenomena may be explained by the Raman selection rules. During the Raman measurements, the radiated SiC-NWs were randomly arranged and had no unique predominant crystalline direction, although the [111] will be the major orientation of growth. Therefore, the polarization of the incident and scattered wave vectors such as the (011) face, which is perpendicular to the quasi-backscattering geometry face (100), was not strictly obeyed.[21,31] Consequently, the TO and LO band lines in the Raman spectrum of our sample were not completely forbidden or allowed but showed a varying intensity ratio with different positions.

The growth of SiC-NWs with a metal catalyst normally results from the VLS mechanism. In the current process, ferrocene was used to serve as the iron catalyst and a source of carbon whereas the silicon wafer was used as a silicon source and the substrate. Here we propose a possible growth model corresponding to the VLS mechanism. During the process, ferrocene [$(C_5H_5)_2Fe$] will favorably be pyrolyzed into iron and carbon at high temperature. The decomposed Fe and C atoms will then be deposited onto the surface of the silicon wafer to form an alloy droplet with Si atoms along the VLS mechanism (Figure 5B, a). Once the Si and C atoms reach supersaturation, the excess atoms will precipitate out from the nuclear (alloy droplet) and grow up to a SiC-NW (Figure 5B, b). In theory, it is also possible for the catalyst to serve as an anchor on the tip of the nanowire. During this step, the one-dimensional SiC-NW structure usually grows along the direction of [111] because of the lowest-energy principle. Here one case should be mentioned; a small quantity of silicon may be oxidized to SiO_2 or SiO. The produced silicon oxide will simultaneously react with the deposited carbon and form the structure of SiC-NW. Furthermore, some silicon or generated silicon oxide will possibly be nitrified by nitrogen gas at high temperature (as shown in Figure 4a). It is noted that the as-formed SiC-NWs are not easy to be nitrified because of their high stability in the present experiments. It is believed that if another inert gas, such as argon, was used, the nitrification will not happen. During the current process, the C, Si, and catalytic Fe sources are supplied simultaneously by ferrocene and the silicon substrate, which obviously simplifies the synthesis process. Thus, a useful technique for synthesizing scales of crystalline SiC-NWs is suggested.

Conclusions

Scales of high-quality crystalline silicon carbide nanowires with small diameters of ≈ 20 nm and lengths of several μms were synthesized by direct thermal evaporation of ferrocene onto a silicon wafer at high temperature. The samples possessed a uniform size, crystalline structure, and a thin oxide layer. The HR-FETEM image showed a main single-crystal direction of [111]. The Raman scattering spectra of the sample showed varying intensity ratios at different positions, which is attributed to the Raman selection rules. Finally, a tentative growth model according to the vapor–liquid–solid (VLS) mechanism was suggested. The simple synthetic process presented here suggests a useful route for the fabrication of crystalline SiC-NWs with high quantity.

Experimental Section

General Procedure: A ceramic boat containing pieces of silicon wafers (n-type Si (100) with a resistivity of about 4.1 Ωcm) and an amount of ferrocene powder was placed on a silicon surface and put in the center of a high-temperature chemical-vapor-deposition furnace. The furnace was heated to 1550 °C at a rate of 10 °C/min. A nitrogen gas flow was initiated at a rate of 70 mL/min at the beginning. After heating for ca. 2 h, the samples were taken out for the next measurements. The morphology and lattice structure of the samples were checked by field emission scanning electric microscopy (FESEM, FEI Sirion) and high-resolution field emission transmission electron microscopy (HR-FETEM, JEM 2010F). The possible chemical composition was investigated by using energy-dispersive X-ray spectroscopy (EDS) attached to the FESEM. The crystalline structure was measured by X-ray diffraction using Cu-K_α radiation (XRD, D8 DISCOVER, Bruker). Raman scattering spectra were measured with a Raman microscope (Renishaw inVia plus) with a 514.5 nm laser as the excitation source at room temperature.

Acknowledgments

This work was supported by the Shanghai-Applied Materials Research and Development Fund (No. 06SA06) and Youth Teacher Fund of Shanghai Jiao Tong University (A2306B). We would like to thank the Instrumental Analysis Center of Shanghai Jiao Tong University for their great help in obtaining the measurements.

[1] J. B. Casady, R. W. Johnson, *Solid-State Electron.* **1996**, *39*, 1409.
[2] Y. Cui, C. M. Lieber, *Science* **2001**, *291*, 851.
[3] C. M. Lieber, *Nano Lett.* **2002**, *2*, 81.
[4] R. Rurali, *Phys. Rev. B* **2005**, *71*, 205405.
[5] H. J. Dai, E. W. Wong, Y. Z. Lu, S. S. Fan, C. M. Lieber, *Nature* **1995**, *375*, 769.
[6] Z. Pan, H. L. Lai, F. C. K. Au, Z. Duan, W. Zhou, W. Shi, N. Wang, C. S. Lee, N. B. Wong, S. T. Lee, S. Xie, *Adv. Mater.* **2000**, *12*, 1186.
[7] Z. J. Li, H. J. Li, X. L. Chen, A. L. Meng, K. Z. Li, Y. P. Xu, L. Dai, *Appl. Phys. A: Mater. Sci. Process* **2003**, *76*, 637.
[8] C. H. Liang, G. W. Meng, L. D. Zhang, Y. C. Wu, Z. Cui, *Chem. Phys. Lett.* **2000**, *329*, 323.
[9] H. K. Seong, H. J. Choi, S. K. Lee, J. I. Lee, D. J. Choi, *Appl. Phys. Lett.* **2004**, *85*, 1256.
[10] B. Yan, G. Zhou, W. Duan, J. Wu, B. Gu, *Appl. Phys. Lett.* **2006**, *89*, 023104.
[11] E. W. Wong, P. E. Sheehan, C. M. Lieber, *Science* **1997**, *277*, 1971.
[12] W. Yang, H. Araki, C. Tang, S. Thaveethavorn, A. Kohyama, H. Suzuki, T. Noda, *Adv. Mater.* **2005**, *17*, 1519.

[13] W. Q. Han, S. S. Fan, Q. Q. Li, W. J. Liang, B. L. Gu, D. P. Yu, *Chem. Phys. Lett.* **1997**, *265*, 374.
[14] A. I. Kharlamov, S. V. Loichenko, N. V. Kirillova, V. V. Fomenko, M. E. Bondarenko, Z. A. Zaitseva, *Inorg. Mater.* **2003**, *39*, 260.
[15] Y. Xia, P. Yang, Y. Sun, Y. Wu, B. Mayers, B. Gates, Y. Yin, F. Kim, H. Han, *Adv. Mater.* **2003**, *15*, 353.
[16] C. C. Tang, S. S. Fan, H. Y. Dang, J. H. Zhao, Z. Zhang, P. Li, Q. Gu, *J. Cryst. Growth* **2000**, *210*, 595.
[17] G. W. Meng, L. D. Zhang, C. M. Mo, S. Y. Zhang, Y. Qin, S. P. Feng, H. J. Li, *J. Mater. Res.* **1998**, *13*, 2533.
[18] Z. X. Yang, Y. D. Xia, R. Mokaya, *Chem. Mater.* **2004**, *16*, 3877.
[19] H. Ye, N. Titchenal, Y. Gogotsi, F. Ko, *Adv. Mater.* **2005**, *17*, 1531.
[20] J. We, K. Z. Li, H. J. Li, Q. G. Fu, L. Zhang, *Mater. Chem. Phys.* **2006**, *95*, 140.
[21] G. Gundiah, G. V. Madhav, A. Govindaraj, M. M. Seikh, C. N. R. Rao, *J. Mater. Chem.* **2002**, *12*, 1606.
[22] X. T. Zhou, N. Wang, H. L. Lai, H. Y. Peng, I. Bello, N. Wong, C. S. Lee, S. T. Lee, *Appl. Phys. Lett.* **1999**, *74*, 3942.
[23] Y. Zhang, N. Wang, R. He, X. Chen, J. Zhu, *Solid State Commun.* **2001**, *118*, 595.
[24] K. Kametani, K. Sudoh, H. Iwasaki, *Thin Solid Films* **2004**, *467*, 50.
[25] H. Y. Kim, J. Park, H. Yang, *Chem. Commun.* **2003**, 256.
[26] K. W. Wong, X. T. Zhou, F. C. K. Au, H. L. Lai, C. S. Lee, S. T. Lee, *Appl. Phys. Lett.* **1999**, *75*, 2918.
[27] W. Yang, H. Miao, Z. Xie, L. Zhang, L. An, *Chem. Phys. Lett.* **2004**, *383*, 441.
[28] Z. S. Wu, S. Z. Deng, N. S. Xu, J. Chen, J. Zhou, J. Chen, *Appl. Phys. Lett.* **2002**, *80*, 3829.
[29] S. Z. Deng, Z. B. Li, W. L. Wang, N. S. Xu, J. Zhou, X. G. Zheng, H. T. Xu, J. Chen, J. C. Lee, *Appl. Phys. Lett.* **2006**, *89*, 023118-1.
[30] H. Okumura, E. Sakuma, J. H. Lee, H. Mukaida, S. Misawa, K. Endo, S. Yoshida, *J. Appl. Phys.* **1987**, *61*, 1134.
[31] S. Zhang, B. Zhu, F. Huang, Y. Yan, E. Shang, S. Fan, W. Han, *Solid State Commun.* **1999**, *111*, 647.
[32] W. Feldman, J. H. Parker Jr, W. J. Choyke, L. Patrick, *Phys. Rev.* **1968**, *173*, 790.
[33] Z. C. Feng, C. C. Tin, R. Hu, J. Willianms, *Thin Solid Films* **1995**, *266*, 1.
[34] D. Olego, M. Cardona, *Phys. Rev. B* **1982**, *25*, 3889.
Received: April 26, 2007
Published Online: July 12, 2007

